Supporting Information

Osmotic pressure triggered cavitation in microcapsules

Luoran Shang,[a] Yao Cheng,[a] Jie Wang,[a] Yunru Yu,[a] Yuanjin Zhao,*[a] Yongping Chen,*[b] and Zhongze Gu*[a]

[a] State Key Laboratory of Bioelectronics, School of Biological Science and Medical Engineering, Southeast University, Nanjing 210096, China.

Email:yjzhao@seu.edu.cn; gu@seu.edu.cn

[b] School of Energy and Environment, Southeast University, Nanjing 210096 , China.

E-mail: ypchen@seu.edu.cn

Experimental

Materials

The surfactant ethylene oxide–propylene oxide–ethylene oxide triblock copolymer (Pluronic F108) and polyvinyl alcohol (PVA), photocurable resin ethoxylated trimethylolpropane triacrylate (ETPTA), the photoinitiator 2–hydroxy–2–methylphenylpropanone (HMPP), the hydrophobic reagent octadecyltrichlorosilane (OTS) and fluorescent polystyrene nanoparticles were all derived from Sigma-Aldrich Co. In order to achieve a better mixing, ETPTA was firstly premixed with ethanol in equal volume. The photoinitiator was then added, with volume fraction of 1% (VHMPP/VETPTA). The mixture was placed in an oven to promote complete volatilization of the ethanol. The ultrafine Fe_2O_3 nanoparticles (50 nm mean diameter) were obtained from Jiangsu Laboratory for Biomaterials and Devices. NaCl was gained from Sinopharm Chemical Reagent Co., Ltd. Deionized water was used in

all experiments.

Microfluidics

The microfluidic device was constructed by assembling glass capillaries on a glass slide. The inner, middle and outer cylindrical capillaries were identical and all gained from World Precision Instruments, Inc. The inner and outer diameters of the capillaries were 580 μm and 1 mm, respectively. The square capillary with an inner diameter of 1.05 mm was purchased from VitroCom, Inc. The inner capillary was tapered using a laboratory portable Bunsen burner (Honest MicroTorch). The Bunsen burner was set in its median thermal power and after 3s heating time; the capillary was stretched by hand to reach a diameter of about 80 μm at the orifice. The middle capillary was tapered by a micropipette puller (Sutter Instrument Co., Novato, USA) and was sanded under optical microscope to reach the desired orifice diameter of about 300μm. For the treatment of the middle capillary, the inner wall was wetted by the hydrophobic reagent octadecyltrichlorosilane (OTS) and incubated for 30 min. After this, the solution was blown out by nitrogen. Then the three capillaries were coaxially and sequentially assembled on a glass slide. To integrate fluids conveniently and to observe the emulsification process, the square capillary was added around the contact area of the middle and outer capillary. The connectors of the assembled capillaries were sealed with dispensing needles and transparent epoxy resin (Devcon 5 Minute Epoxy) where necessary.

Microcapsules generation and Cavitation

The inner and middle phases flowed through the inner and middle capillary respectively in the same direction. The continuous phase flowed via the interstices between the square capillary and the middle capillary, or between the square capillary and the outer capillary. The inner phase was an aqueous solution of surfactant (Pluronic F108, 2 wt%). The middle oil phase was a photocurable resin (ETPTA) with 1vol% photoinitiator HMPP. The outer phase was a mixture of two surfactant solutions (2wt% F108 and 10wt% PVA, with volume ratio of 2:1). Each fluid was pumped by a syringe pump (Harvard PHD 2000 Series), and was connected through a polyethylene tube(Scientific Commodities

Inc., with inner and outer diameters of 0.86 mm and 1.32 mm, respectively.) with a glass syringe(SGE Analytical Science). The three phases were induced to the microfluidic device in a sequential co-flow regime and double emulsions were generated in the outer capillary. The droplets were solidified downstream upon *in situ* UV irradiation for 3s by a UV-light (EXFO OmniCure SERIES 1000, 365nm, 100W). The as-prepared microcapsules were then immersed in NaCl solution at room temperature.

Characterization

The emulsification process in the collection capillary of the device was observed in real time under an inverted microscope (AE2000, Motic) and was recorded by a charged coupled device (CCD, S-PRI F1, AOS Technologies AG). The optical images of the microcapsules and microbubbles were observed by a stereomicroscope (NOVEL NTB-3A, Ningbo Yongxin Optics Co., Ltd, China) and were captured by a CCD (Media Cybernetics Evolution MP 5.0 RTV). The outer radius (R_{outer}), inner radius (R_{inner}), and shell thickness (h) of the microcapsules were all measured by software Image-Pro Plus 7.0. Shell thickness was calculated from R_{outer} minus R_{inner}. Each set of experiments were repeated five times and the average values were gained. The capsules evolution process was monitored under the same stereomicroscope and images and movies were captured by the same CCD afore mentioned. Fluorescence photographs of the microbubbles were taken by a Laser Scanning Confocal Microscope (Carl Zeiss, LSM510). The microstructures of ruptured microcapsules were characterized by a scanning electron microscope (SEM, HITACHI, S-3000N).

Magnetically-controlled motion

The ultrafine Fe_2O_3 nanoparticles (50 nm mean diameter) were dispersed into the middle oil phase in the microfluidic system. Microcapsules with magnetic shells were then prepared and went through the same evolution process as described before. Thus, microbubbles with magnetic polymer shell were generated. The magnetic particles were then pulled to one side of a vial by using a permanent magnet.

Ultrasound imaging

The in vitro acoustic imaging experiment was carried out through a B-mode diagnostic ultrasonic system (VEVO 2100, FujiFilm VisualSonics Inc.), which was composed of an ultrasonic probe, a self-prepared phantom simulating human acoustic features and a digital instrument for images display and storage. The phantom was prepared by mixing agar, glycerin and deionized water (with mass ratio of 3: 4: 90). The mixture was sufficiently stirred and heated to 90 ^{o}C and stood for over half an hour until it became transparent and sticky. Then, it was poured into a glass container with a sound-absorbing sponge at the bottom. To mimic human blood vessel, a silicone tube was inserted and was later extracted when the mixture was completely solidified. The particle suspension was then injected to the channel. Ultrasound signal was generated by an ultrasound probe (18 MHz) and the contrast images were picked up and displayed on the computer screen.

Supporting Figures:

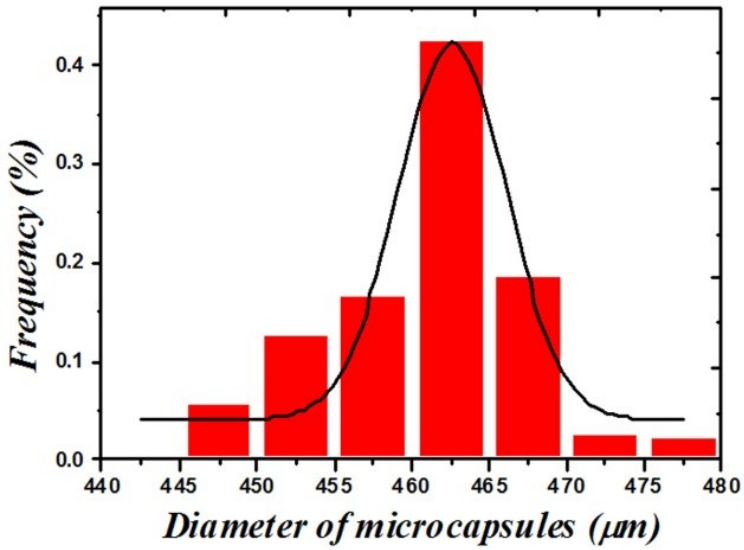

Figure S1. The statistical size distribution histogram of the microfluidic-prepared microcapsules. The flow rates of the inner, middle and outer phases were set to be 0.08ml/h, 1ml/h, and 5ml/h, respectively. The sizes of particles were narrowly distributed within the range of 440μm to 480μm. The standard deviation and the average diameter were calculated to be 6.62 and 460.79, respectively. Thus, the coefficient of variation (CV), of the particles, which is defined as the quotient of the standard deviation by the average diameter of the particles, was calculated to be 1.44%. These results confirmed that the microfluidic-prepared particles were highly monodisperse.

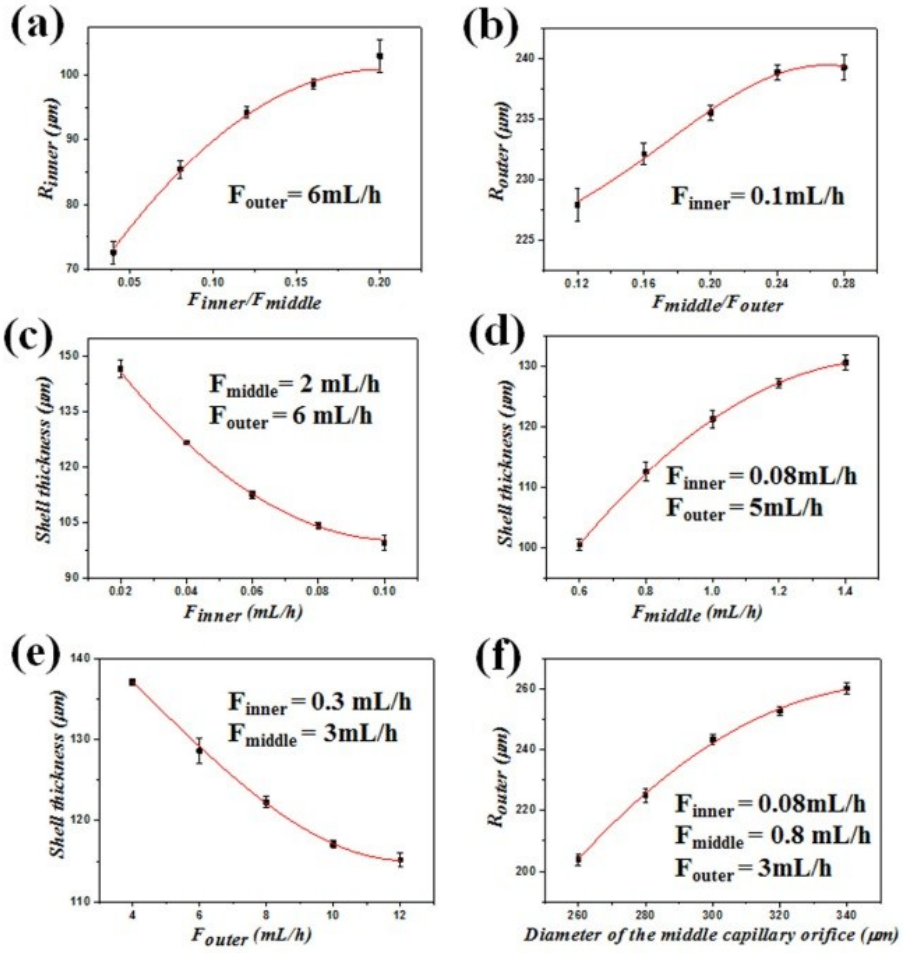

Figure S2. The relationships between experimental variables (flow rates and device dimension) and the diameter of microcapsules as well as shell thickness. The insets annotate the flow rates: (a) the inner radius of the microcapsules (R_{inner}) increased with the ratio of the inner and middle flow rates (F_{inner}/F_{middle}); (b) the outer radius of the microcapsules (R_{outer}) increased with the ratio of middle and outer flow rates (F_{middle}/F_{outer}); (c–e) the average shell thickness of the drops increase with F_{middle}; while decrease with increase of F_{inner} or F_{outer}; (f) at the given set of flow rates, R_{outer} increased with the diameter of the middle capillary orifice. R_{outer} increased with the diameter of the middle capillary orifice.

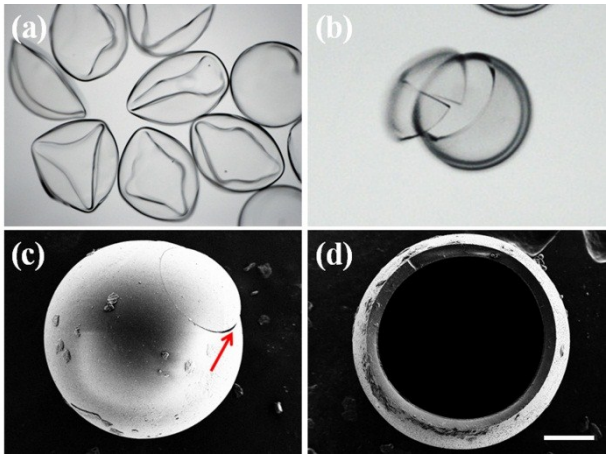

Figure S3. The folded and ruptured microcapsules: (a) microscope photograph of the folded microcapsules; (b) microscope photograph of a ruptured microcapsule; (c) SEM image of a cracked microcapsule. The red row indicated the cleft; (c) SEM image of a microcapsule after a complete bursting. The capsule seemed like been torn in half and the ruptured part of the shell was detached from the main part of the capsules. Scale bar is 100μm.

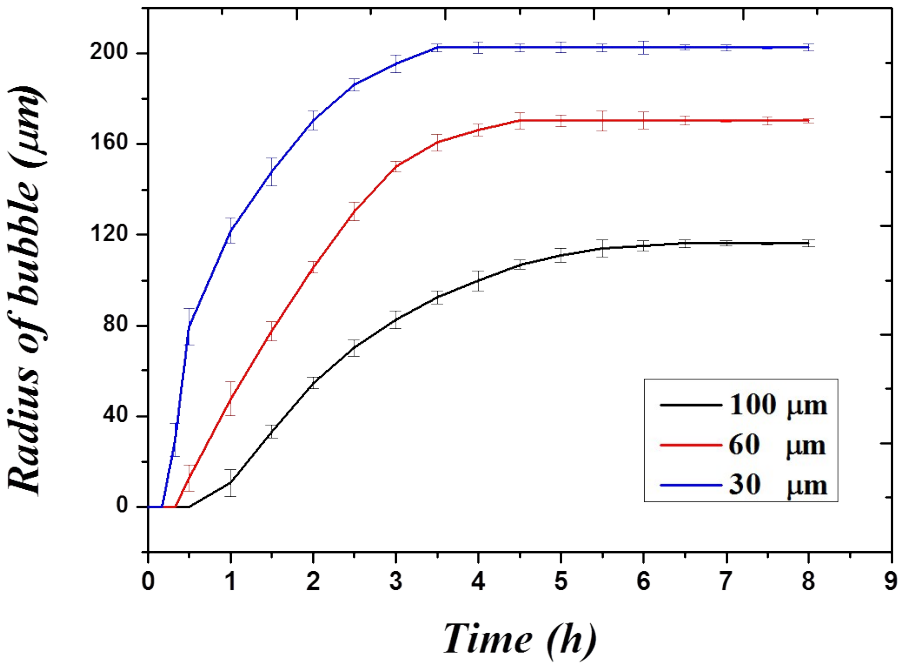

Figure S4. The relationships between treatment time of the microcapsules and the radius of the generated microbubbles. The bubble grew continuously over time and reached an ultimate diameter value, which was pre-determined by the diameter of the original water-filled microcapsules. With other variables constant, bubble emerged at an earlier time and grew faster in capsules with a thinner shell.

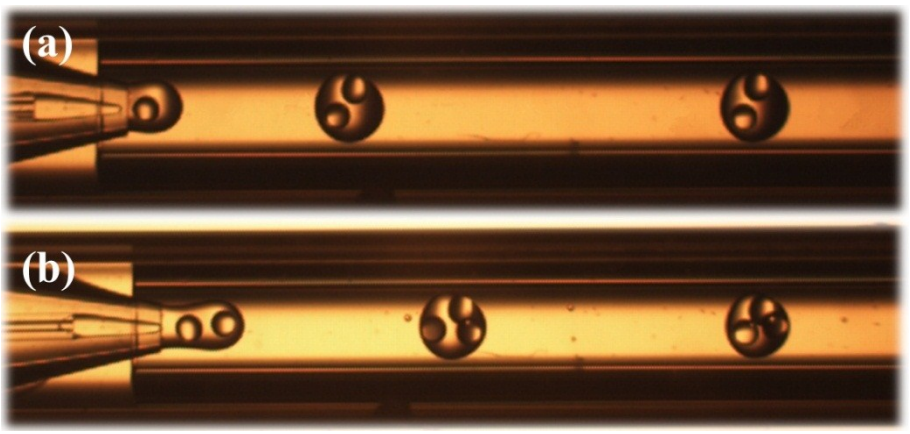

Figure S5. Real-time images of the microfluidic fabrication of double emulsion templates with two (a) and three (b) cores, respectively.

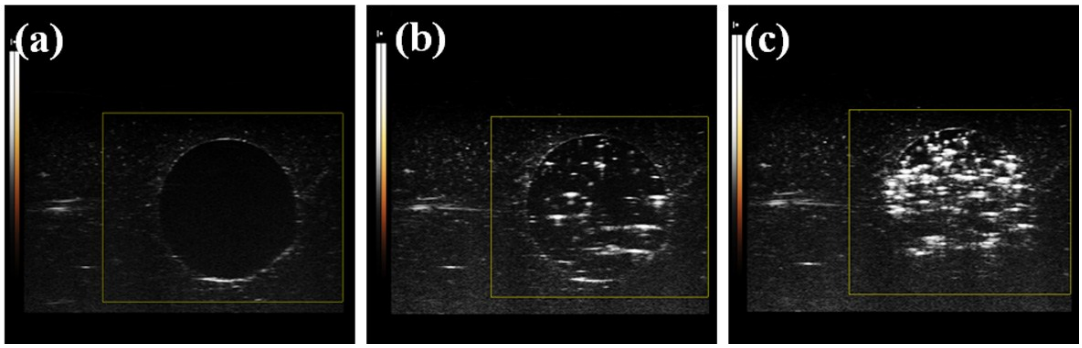

Figure S6 B-mode ultrasound images of: (a) distilled water as a blank control; (b, c) microbubbles with low concentration and high concentration, respectively. It can be found that the ultrasonic contrast signal was enhanced by the microbubbles. The yellow rectangular boxes marked the region of interest (ROI).

Supporting Movies:

Movie S1 Buckling and the bubble occurrence process of microcapsules with a medium thickness of ETPTA shell.

Movie S2 Bubble occurrence and growth process of microcapsules with a thick ETPTA shell.